CAMBRIDGE
UNIVERSITY PRESS

Article

Progress in the knowledge of 'ruby silvers': New structural and chemical data of pyrostilpnite, Ag₃SbS₃

Cristian Biagioni[1]* , Federica Zaccarini[2], Philippe Roth[3] and Luca Bindi[4]

[1]Dipartimento di Scienze della Terra, Università di Pisa, Via Santa Maria 53, 56126 Pisa, Italy; [2]Department of Applied Geological Sciences and Geophysics, University of Leoben, Peter Tunner Str. 5, A-8700 Leoben, Austria; [3]Swiss Seismological Service, ETH Zurich, Sonneggstr. 5, 8092 Zurich, Switzerland; and [4]Dipartimento di Scienze della Terra, Università degli Studi di Firenze, via La Pira 4, I-50121 Firenze, Italy

Abstract

The crystal structure of pyrostilpnite from the Plaka mine, Lavrion Mining District, Greece, was refined in the space group $P2_1/c$ to a final R_1 index of 0.0283 on the basis of 2047 reflections with $F_o > 4\sigma(F_o)$ and 65 refined parameters. Unit-cell parameters of the crystal examined are $a = 6.8629(6)$, $b = 15.8800(14)$, $c = 6.2711(5)$ Å, $\beta = 117.087(2)°$, $V = 608.48(9)$ Å^3 and $Z = 4$. Chemical data agree with the stoichiometric formula Ag₃SbS₃. The crystal structure reported previously was confirmed, although a higher precision of refinement was achieved. It can be described as formed by {010} slabs running along **c** and connected along **a** through relatively longer Ag–S bonds. The analysis of the atomic displacement parameters together with a refinement with higher order tensors in the expression of the structure factors revealed no hint for pyrostilpnite as an ionic conductor. A historical background of the 'ruby silvers' is also reported.

Introduction

The name 'ruby silvers' was used by miners to indicate the reddish minerals that were often found in silver deposits. In the first half of the 19th century it was recognised that this material could be traced back to four different species – very similar to each other, not only in appearance, but also in the chemical composition, as they consisted of 'sulfoarsenite' or 'sulfoantimonite' of silver (Ag₃AsS₃–Ag₃SbS₃) – in two polymorphic series, the trigonal one, formed by proustite and pyrargyrite, and the monoclinic one, consisting of xanthoconite and pyrostilpnite. This work deals with the revision of the crystal structure of pyrostilpnite, Ag₃SbS₃.

Historical background of 'ruby silvers'

The minerals belonging to the proustite–pyrargyrite series are widespread in Nature. As reported in the historical introduction in the treatise of Hintze (1904), these minerals were already known by Agricola in the 16th century with the name of *argentum rude rubrum* and probably even earlier, in the 14th century, by Basilio Valentino with the name of *Rothgiltigerz*, a corruption of *Roth Gültigerz* (which could translate into 'valuable red ore'), which was then even more corrupted as *Rothgolderz* or *Rothguldenerz* (i.e. 'red gold ore') suggesting the presence of gold. However, it was the nature of the silver minerals that was confirmed, not only by Agricola, but by all subsequent scholars, such as Gesner and Henckel, who also reported the presence of arsenic. Slight differences in appearance were also noted, such

that Wallerius, in 1747, and Werner in 1789, distinguished the mineral as 'dunkles' (i.e. dark) and 'lichtes' (i.e. clear). The reason for this distinction was explained by the chemical analyses carried out by Proust in 1804, who verified not only the absence of oxygen, indicated by the first analysts (Bergmann in 1780, Klaproth in 1795, Vauquelin in 1796 and Thenard in 1800), but that the dark material contained Ag, Sb and S whereas the clear one showed Ag, As and S, and only rarely was there the simultaneous presence of As and Sb. Nonetheless, Mohs, in 1824, continued to think of a single mineral that he called *Rubinblende* attributing the two different colour tones to varieties. In 1827 Breithaupt reiterated that there were two different species, that he named *Arsensilberblende* and *Antimonsilberblende*. *Antimonsilberblende* was then renamed by Glocker in 1831 as pyrargyrite (from the Greek 'silver of fire') and was accepted by the mineralogical community despite a new proposal by Beudant in 1832 for the name *Argyrithrose* ('silver rose'). However, the French scholar was successful with the proposal for naming the As-rich species with the name proustite, in homage to the great chemist Joseph-Louis Proust (1754–1826), who first recognised the existence of the two different species and who discovered the fundamental chemical law of 'definite proportions'.

The fortunate occurrence of the discovery of beautiful crystals of both species allowed accurate crystallographic determinations. Haüy in 1801 and Mohs in 1824 found many simple crystal forms that later, thanks also to the systematic work of Quintino Sella of 1856, summed to 94 plus another 50 uncertain forms. The symmetry appeared to be trigonal, then specified in 3*m*, ditrigonal pyramidal class, after the initial assignment to the rhombohedral one.

The discovery by Breithaupt, in 1832, of crystals from the mines of Freiberg in Saxony with a clearly lower symmetry was

*Author for correspondence: Cristian Biagioni, Email: cristian.biagioni@unipi.it

a surprise. He called them *Feuerblende* ('fire blende' due to the similarity with common sphalerite). Goniometric measurements led Kenngott in 1849 to assign an orthorhombic symmetry, but then Roemer in 1848 and Miller in 1852 established the prismatic monoclinic $2/m$ symmetry. The species was later named pyrostilpnite ('shining fire') by Dana in 1868, a name generally accepted. Breithaupt himself in 1840 had identified another species among the samples from the collection of the Freiberg museum (collected in a mine near the town in 1797), that he called *Xanthokon* (i.e. 'yellow powder') showing an identical composition to that of proustite, a name which was later standardised by Dana in 1868 as xanthoconite. Determinations in 1866 by Weissbach on larger crystals with apparent hexagonal morphology proved that they had prismatic monoclinic symmetry. Thus, these two silver sulfosalts were established as a polymorphic pair.

Subsequent structural research (Engel and Nowacki, 1966) asserted the isotypism of proustite and pyrargyrite in the space group $R\bar{3}c$ and confirmed Harker's first determination of 1936. The other pair has two different space groups, $C2/c$ for xanthoconite and $P2_1/c$ for pyrostilpnite, as determined by Engel and Nowacki (1968) and Kutoglu (1968), respectively. Whereas the crystal structures of pyrargyrite, proustite, and xanthoconite were refined down to satisfying R values, the structure refinement of pyrostilpnite was of relatively low quality (R = 15.1% – Kutoglu, 1968). In the framework of a systematic study of silver sulfosalts (e.g. Bindi and Biagioni, 2018), a new crystallographic investigation of this mineral was performed, improving the quality of the available structural data.

Material studied

The pyrostilpnite specimen, belonging to the private collection of one of us (PR) and used for the chemical and structural study, comes from the Plaka mine, Lavrion Mining District, Greece. At Plaka the ore system is genetically related to the emplacement of a Miocene biotite ± hornblende granodioritic body and granodiorite porphyry dykes/sills within metamorphic Mesozoic rocks of the Attic–Cycladic Crystalline Belt (Voudouris *et al.*, 2008). The ore system is composed of vein-type ores enriched in Mo, W, Pb, Zn, Cu, As, Sb, Bi and Ag. The more common minerals at the deposit are: pyrrhotite, chalcopyrite, arsenopyrite, sphalerite (both Fe-rich and Fe-poor), löllingite, Ag-rich tetrahedrite, bournonite, pyrargyrite, pyrostilpnite, miargyrite, native arsenic, semseyite, heteromorphite, veenite, falkmanite, fluorite, quartz and siderite. According to Wendel and Rieck (1999), a set of As-rich veins was first formed at temperatures between 320 and 150°C, while a later stage associated with Sb-rich mineralisation occurred at lower temperatures.

The crystals investigated were found in January 1999 in the Plaka mine no. 80 ('Filoni 80'), one of the several interconnected Plaka mines. Pyrostilpnite occurred primarily as prismatic crystals with typical monoclinic terminations but also as pseudohexagonal crystals. Crystal size is up to 0.7 mm across. On the specimen investigated pyrostilpnite is associated with proustite and secondary arsenates. Fluorite and native antimony are also part of the association (Wendel and Rieck, 1999).

Chemical data

The chemical composition of the pyrostilpnite crystal used for the structural study (see below) was first qualitatively analysed with

Table 1. Summary of crystal data and parameters describing data collection and refinement for pyrostilpnite.

Crystal data	
Chemical formula	Ag_3SbS_3
Crystal size (mm)	$0.100 \times 0.080 \times 0.075$
Cell setting, space group	Monoclinic, $P2_1/c$
a (Å)	6.8629(6)
b (Å)	15.8800(14)
c (Å)	6.2711(5)
β (°)	117.087(2)
V (Å^3)	608.48(9)
Z	4
Data collection and refinement	
Radiation, wavelength (Å)	Mo$K\alpha$, λ = 0.71073
Temperature (K)	293(3)
$2\theta_{max}$ (°)	66.24
Measured reflections	14,626
Unique reflections	2097
Reflections with $F_o > 4\sigma(F_o)$	2047
R_{int}	0.0347
$R\sigma$	0.0234
Range of h, k, l	$-10 \leq h \leq 10$, $-24 \leq k \leq 24$, $-9 \leq l \leq 8$
R [$F_o > 4\sigma(F_o)$]	0.0282
R (all data)	0.0292
wR (on F_o^2)	0.0629
Goof	1.112
No. of least-squares parameters	65
$\Delta\rho_{max}$, $\Delta\rho_{min}$ (e^- Å^{-3})	1.55 (at 0.48 Å from Sb) −1.27 (at 0.91 Å from Ag3)

energy-dispersive X-ray spectroscopy (EDS). The analyses did not indicate the presence of elements ($Z > 9$) other than Ag, Sb and S. Quantitative wavelength-dispersive X-ray (WDS) analyses (n = 2) were obtained using a JEOL-JXA 8200 microprobe, installed in the E. F. Stumpfl laboratory (Leoben University, Austria), operating in WDS mode. Analytical conditions were: 20 kV, 10 nA and 1 μm beam size, with counting times of 15 s on-peak and 5 s for each background position. Standards used were: electrum for Ag (Ag$L\alpha$) and stibnite for Sb and S (Sb$L\beta$ and S$K\alpha$). The crystal fragment was found to be chemically homogeneous within the uncertainty of our measurements (Ag 59.20–59.98; Sb 22.24–22.27; and S 17.68–17.94 wt.%). The empirical formula, based on $\Sigma(Ag + Sb) = 4$ atoms per formula unit, is Ag$_{3.00–3.01}$Sb$_{0.99–1.00}$S$_{3.02–3.03}$.

X-ray crystallography

Single-crystal X-ray diffraction intensity data were collected on pyrostilpnite using a Bruker Smart Breeze diffractometer (50 kV and 30 mA) equipped with a Photon II CCD detector and graphite-monochromatised Mo$K\alpha$ radiation (Earth Science Department, University of Pisa). The detector-to-crystal distance was set at 50 mm. Data were collected using ω scan mode in 0.5° slices, with an exposure time of 10 s per frame, and they were corrected for Lorentz and polarisation factors as well as for absorption using the software package *Apex3* (Bruker AXS Inc., 2016). The refined unit-cell parameters are a = 6.8629(6), b = 15.8800 (14), c = 6.2711(5) Å, β = 117.087(2)°, V = 608.48(9) Å^3 and Z = 4; space group $P2_1/c$. The crystal structure was refined using *Shelxl-2018* (Sheldrick, 2015) starting from the atomic coordinates given by Kutoglu (1968). Scattering curves for neutral atoms were taken from the *International Tables for Crystallography* (Wilson, 1992). Twinning according to a two-fold axis along [001] was

Table 2. Sites, fractional atomic coordinates and equivalent isotropic displacement parameters (Å²) for pyrostilpnite.

Atom	x/a	y/b	z/c	U_{eq}
Ag1	0.03667(11)	0.31355(4)	0.26401(13)	0.04341(15)
Ag2	0.47170(13)	0.24028(4)	0.28353(13)	0.04739(17)
Ag3	−0.40374(8)	0.09234(4)	0.05492(11)	0.03853(13)
Sb	0.19754(6)	0.05211(2)	0.37670(7)	0.01776(7)
S1	0.21834(2)	0.05960(9)	−0.0043(2)	0.0202(2)
S2	−0.4626(2)	0.13633(9)	0.5972(2)	0.0207(2)
S3	−0.0558(2)	0.16695(9)	0.3177(3)	0.0225(3)

Table 3. Selected bond distances (Å) for pyrostilpnite.

Ag1–S1^i	2.4645(15)	Ag1–Ag2	3.1543(10)
Ag1–S2^{ii}	3.1943(15)	Ag1–Ag2^i	3.3765(11)
Ag1–S3	2.4760(16)		
Ag1–S3^{ii}	2.5911(18)	Ag2–Ag2^i	3.1507(3)
		Ag2–Ag2^{ii}	3.1507(3)
Ag2–S2^{iii}	2.4265(15)	Ag2–Ag3^v	3.0605(10)
Ag2–S2^{iv}	2.4472(16)	Ag2–Ag3^{iv}	3.0695(9)
Ag3–S1^{vi}	2.5013(15)	Ag3–Ag3^{ix}	3.1611(11)
Ag3–S1^{viii}	2.8123(15)		
Ag3–S2^{vii}	2.7993(16)	Sb–S1	2.4606(14)
Ag3–S3	2.4976(15)	Sb–S2^{iv}	2.4907(14)
		Sb–S3	2.4288(15)

Symmetry codes: (i) x, −y + 1/2, z + 1/2; (ii) x, −y + 1/2, z−1/2; (iii) x + 1, −y + 1/2, z−1/2; (iv) x + 1, y, z; (v) x + 1, −y + 1/2, z + 1/2; (vi) x−1, y, z; (vii) x, y, z−1; (viii) −x, −y, −z; (ix) −x−1, −y, −z.

Table 4. Bond-valence sums (in valence unit) for pyrostilpnite.

Site	Ag1	Ag2	Ag3	Sb	Σanions	Theoretical
S1	0.43		0.39, 0.17	0.97	1.96	2.00
S2		0.47, 0.45	0.17	0.90	1.99	2.00
S3	0.41, 0.30		0.39	1.06	2.16	2.00
Σcations	1.14	0.92	1.12	2.93		
Theoretical	1.00	1.00	1.00	3.00		

modelled, giving a twin ratio of 72:28. After several cycles of refinement using anisotropic displacement parameters for all the atoms, the structural model converged to $R_1 = 0.0283$ for 2047 reflections with $F_o > 4\sigma(F_o)$ and 65 refined parameters. Details of data collection and refinement are given in Table 1. Fractional atomic coordinates and equivalent isotropic displacement parameters are reported in Table 2. Table 3 reports selected bond distances and Table 4 gives the bond-valence calculations obtained using the bond-valence parameters of Brese and O'Keeffe (1991). The crystallographic information files have been deposited with the Principal Editor of *Mineralogical Magazine* and are available as Supplementary material (see below).

Results and discussions

Crystal structure description and relationship with xanthoconite

Apart from a better precision of the refinement, this structural study showed pyrostilpnite to have the same topology previously reported by Kutoglu (1968). The crystal structure of pyrostilpnite
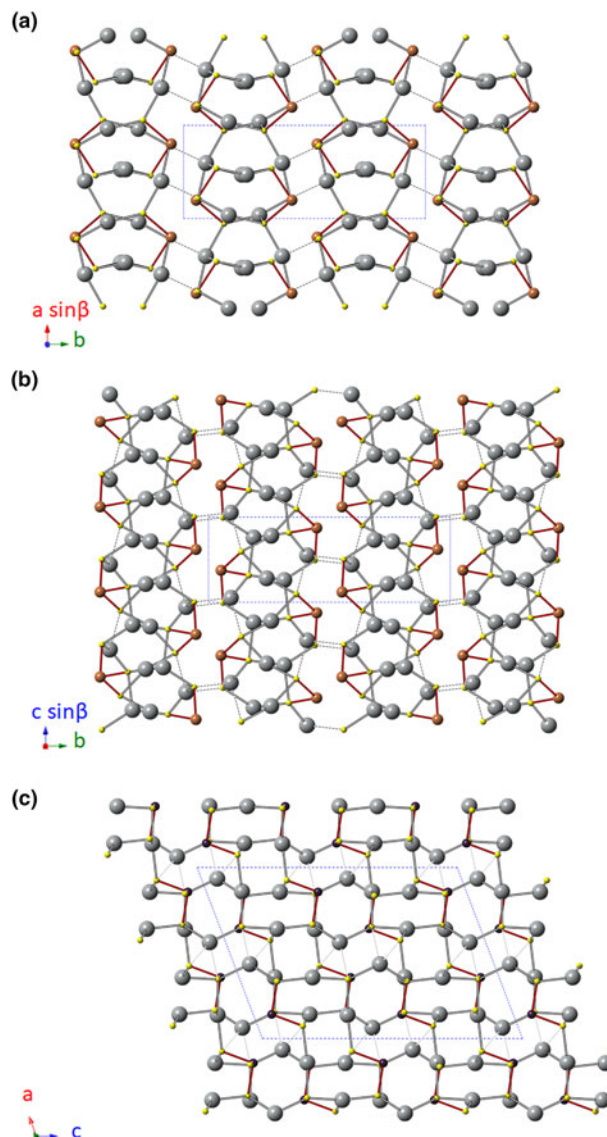

Fig. 1. Crystal structure of pyrostilpnite as seen down **c** (*a*) and **a** (*b*). For the sake of comparison, the crystal structure of xanthoconite is shown in (*c*), as seen down **b**. Grey, brownish, violet, and yellow circles indicate Ag, Sb, As and S atoms, respectively. Thick lines indicates short Ag–S (grey) and (Sb/As)–S (red) bonds, whereas dotted grey lines indicate longer Ag–S bonds. The unit cell is shown with dashed lines.

(Fig. 1*a,b*) shows three independent Ag sites, one Sb position and three S sites.

Silver atoms show different kinds of coordination. Ag1 has a planar triangular coordination, with an average bond distance of 2.511 Å. An additional longer bond at 3.19 Å increases the coordination number to four. Ag2 has a linear coordination, with an average bond distance of 2.437 Å and an S2–Ag2–S2 angle of 157.69(7)°. Finally, Ag3 shows a tetrahedral coordination, with two shorter distances (∼2.50 Å), in a quasi-linear geometry [S1–Ag3–S3 angle of 144.26(5)°] and two longer ones (∼2.50 Å). Bond-valence sums (BVS) at the Ag sites agree with their full-occupancy by Ag atoms, ranging between 0.92 and 1.14 valence units (vu). In the high-T polymorph pyrargyrite, Ag has a linear coordination, with two distances at ∼2.45 Å; the coordination sphere is completed by two additional longer

bonds, at 2.88 and 3.16 Å (Laufek *et al.*, 2010). In the related mineral xanthoconite, Ag_3AsS_3, Ag atoms have a three-fold or four-fold coordination. Three-fold coordinated Ag sites have an additional longer bond, with Ag–S distance longer than 3 Å (Engel and Nowacki, 1968; Rosenstingl and Pertlik, 1993). Similar features can be observed in eckerite, $CuAg_2AsS_3$ (Bindi *et al.*, 2015). Antimony atoms are hosted at the Sb site, showing the typical trigonal pyramidal coordination, with an average bond distance of 2.460 Å and BVS of 2.93 vu.

Taking into account the strongest *Me*–S bonds, the crystal structure of pyrostilpnite can be described as formed by {010} slabs running along **c** (Fig. 1). These slabs are connected through relatively weak Ag3–S1 bonds (2.81 Å). Within the slabs, Ag2, having a linear coordination, forms zig-zag chains running along **c**. Antimony atoms decorate the slabs, with their lone-electron-pair protruding in the space between successive slabs along **b**. This layered organisation is in keeping with the flattened {010} morphology of pyrostilpnite and the occurrence of laths elongated parallel to [001] (Anthony *et al.*, 1990). In addition, the {010} planes of weakest bonds may correspond to cleavage planes in pyrostilpnite. Finally, the twinning of the studied crystal according to a two-fold axis along [001], as revealed by the structural study, agrees with classic data that indicate a twin on {100} with (100) as the composition plane (e.g. Anthony *et al.*, 1990).

Figure 1c shows a projection, along **b**, of the crystal structure of the chemically related mineral xanthoconite. Notwithstanding some similarities between the projection of the general organisation of the {010} layers of pyrostilpnite along **c** (Fig. 1a) and the {001} layers in xanthoconite (Fig. 1c) as seen along **b**, many differences related to the layer stacking, the orientation of the *Me*S_3 pyramids (*Me* = Sb and As in pyrostilpnite and xanthoconite, respectively), and the Ag coordinations can be observed. In addition, whereas Fig. 1a shows an undulated layered organisation in pyrostilpnite, such a feature is lacking in xanthoconite. Consequently, contrary to what was reported by Moëlo *et al.*

(2008), pyrostilpnite and xanthoconite are neither isotypes nor homeotypes.

Pyrostilpnite in the frame of ion conductors

Silver- and Cu-bearing sulfosalts are a very important class of disordered structures (Bindi and Biagioni, 2018). In most of these structures disorder is commonly observed during the structure solution mainly because of orbital mixing and polarisation factors of d^{10}-cations (i.e. Ag^+ and Cu^+ ions), which can result in the formation of various complex asymmetric coordinations often producing overlapping sites (Gaudin *et al.*, 2001). Classic examples of this kind of mineral are samsonite, $Ag_4MnSb_2S_6$ (Bindi and Evain, 2007), stephanite, Ag_5SbS_4 (Leitl *et al.*, 2009), pearceite–polybasite group minerals, [$(Ag,Cu)_{16}MS_{11}$ where M = Sb or As] (i.e. Bindi *et al.* 2006, 2007a,b), proustite, Ag_3AsS_3 (Gagor *et al.*, 2009) and pyrargyrite, Ag_3SbS_3 (Laufek *et al.*, 2010). The structures of these minerals have been efficiently described with the so-called 'non-harmonic approach', which represents an alternative way to describe disordered materials than the classical approach based on the split-atom model. Bindi and Evain (2007) demonstrated that the non-harmonic approach based on Gram–Charlier development of the atomic displacement factors (Kuhs, 1992) represents an alternative and more effective way to determine and describe the structure of these disordered minerals. This approach is especially indicated to refine structures with high isotropic thermal parameters for the Ag or Cu atoms, responsible for the presence of strong ionic conductivity as the activation energy of the jumps from site to site is lowered by the easy electron density deformation.

Among 'ruby silvers', proustite (Gagor *et al.*, 2009) and pyrargyrite (Laufek *et al.*, 2010) have been restudied with the non-harmonic approach based on Gram–Charlier development of the atomic displacement factors. In both cases, the introduction of third-order non-harmonic Gram–Charlier tensors for the Debye–Waller description of Ag atoms led to a significant
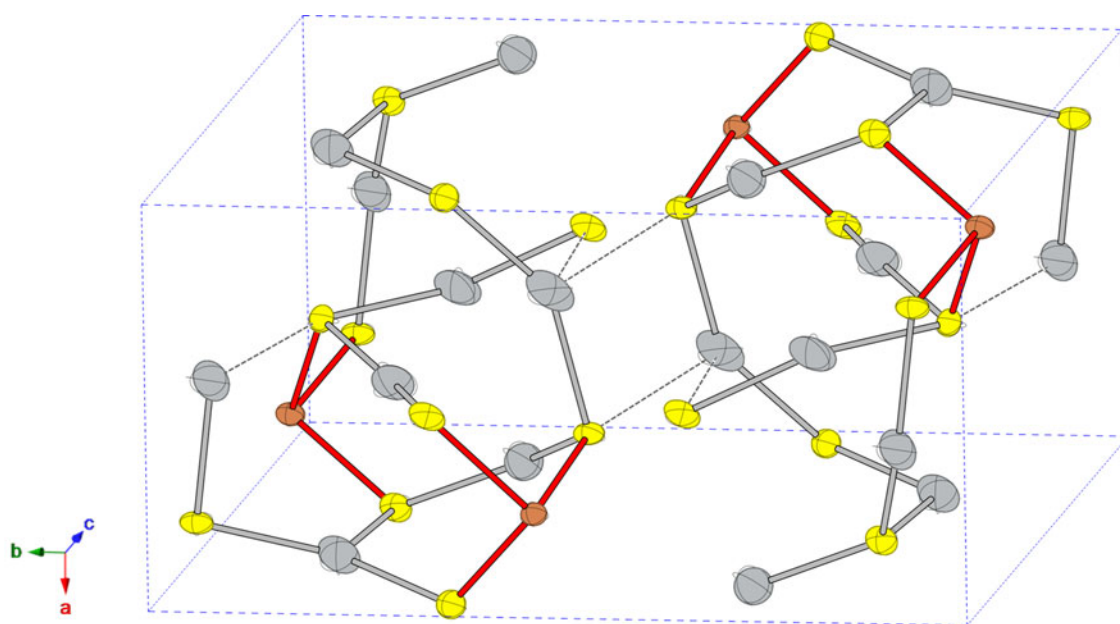

Fig. 2. Unit-cell content of pyrostilpnite, shown as displacement ellipsoids (50% probability level). Grey, brownish, and yellow ellipsoids represent Ag, Sb and S atoms, respectively.

decrease in the R factor and to a considerable drop of residuals in the difference-Fourier maps. The non-harmonic refinement of both proustite and pyrargyrite pointed out the roughly triangular shape of electron density centred around the Ag atoms. In detail, two of the Ag atoms in the structure of these minerals are located on the same Ag–S–Ag spiral running along the three-fold **c**-axis, whereas the third Ag atom is located on the neighbouring spiral. This behaviour is symptomatic of an ionic conduction where the Ag transfer is possible either within the Ag–S–Ag spirals and Ag–Ag chains or between these spirals and chains.

The crystal structure of the pyrostilpnite studied here was refined with the classic approach (Gaussian approximation of the atomic displacement factors). Although the U_{eq} of Ag atoms are 2–3 times larger than Sb/S atoms, no significant residuals were found in the difference-Fourier maps or signs of particular displacements of the atomic displacement parameters indicating a diffusion path (Fig. 2). This feature, together with the absence of a real structural disorder, seemed to rule out the use of the non-harmonic approach based on Gram–Charlier development of the atomic displacement factors. Notwithstanding, we tried to refine the structure with this procedure.

The refinement, carried out with *JANA2006* (Petříček *et al.*, 2006) and using third-order non-harmonic Gram–Charlier tensors for the Debye–Waller description of Ag1 and Ag2 atoms (the Ag atoms having the largest U_{eq}), showed negative regions in the probability density functions, which indicated the inadequacy of the results. The structural results seem to indicate that if an ionic conduction does exist for pyrostilpnite, it should be exceedingly low. This is in agreement with the fact that pyrostilpnite is the low-temperature polymorph of Ag_3SbS_3. The lower the temperature of formation of the mineral, the lower its ionic conductivity.

It will be interesting to study pyrostilpnite by means of X-ray single-crystal diffraction experiments at high temperature. A transition to a fast ion conduction form could be reached, with Ag ions disordered to form a so-called 'molten sublattice'. Such a transition has been observed in both proustite and pyrargite at ∼540 and 490 K, respectively (Schönau and Redfern, 2002). Such experiments are currently under investigation.

References

Anthony J.W., Bideaux R.A., Bladh K.W. and Nichols M.C. (1990) *Handbook of Mineralogy. Volume I. Elements, Sulfides, Sulfosalts*. Mineral Data Publishing, Tucson, Arizona, 588 p.

Bindi L. and Biagioni C. (2018) A crystallographic excursion in the extraordinary world of minerals: The case of Cu- and Ag-rich sulfosalts. *Acta Crystallographica*, **B74**, 527–538.

Bindi L. and Evain M. (2007) Gram–Charlier development of the atomic displacement factors into minerals structures: the case of samsonite $Ag_4MnSb_2S_6$. *American Mineralogist*, **92**, 886–891.

Bindi L., Evain M., Pradel A., Ribes A. and Menchetti S. (2006) Fast ion conduction character and ionic phase-transitions in disordered crystals: the complex case of the minerals of the pearceite–polybasite group. *Physics and Chemistry of Minerals*, **33**, 677–690.

Bindi L., Evain M., Spry P.G., Tait K. and Menchetti S. (2007a) Structural role of copper in the minerals of the pearceite–polybasite group: the case of the new minerals cupropearceite and cupropolybasite. *Mineralogical Magazine*, **71**, 641–650.

Bindi L., Evain M. and Menchetti S. (2007b) Complex twinning, polytypism and disorder phenomena in the crystal structures of antimonpearceite and arsenpolybasite. *The Canadian Mineralogist*, **45**, 321–333.

Bindi L., Nestola F., Graeser S., Tropper P. and Raber T. (2015) Eckerite, Ag_2CuAsS_3, a new Cu-bearing sulfosalt from Lengenbach quarry, Binn valley, Switzerland: description and crystal structure. *Mineralogical Magazine*, **79**, 687–694.

Brese N.E. and O'Keeffe M. (1991) Bond-valence parameters for solids. *Acta Crystallographica*, **B47**, 192–197.

Bruker AXS Inc. (2016) *APEX 3*. Bruker Advanced X-ray Solutions, Madison, Wisconsin, USA.

Engel P. and Nowacki W. (1966) Die Verfeinerung der Kristallstruktur von Proustit, Ag_3AsS_3, und Pyrargyrit, Ag_3SbS_3. *Neues Jahrbuch für Mineralogie, Monatshefte*, **1966**, 181–184.

Engel P. and Nowacki W. (1968) Die Kristallstruktur von Xanthocon, Ag_3AsS_3. *Acta Crystallographica*, **B24**, 77–81.

Gagor A., Pawtowski A. and Petrazsko A. (2009) Silver transfer in proustite Ag_3AsS_3 at high temperatures: conductivity and single-crystal X-ray studies. *Journal of Solid State Chemistry*, **182**, 451–456.

Gaudin E., Boucher F. and Evain M. (2001) Some factors governing Ag^+ and Cu^+ low coordination in chalcogenide environments. *Journal of Solid State Chemistry*, **160**, 212–221.

Hintze C. (1904) *Handbuch der Mineralogie, I, 1*. Verlag von Veit & Comp, Leipzig, Germany, pp. 1208.

Kuhs W.F. (1992) Generalized atomic displacements in crystallographic structure analysis. *Acta Crystallographica*, **A48**, 80–98.

Kutoglu A. (1968) Die Struktur der Pyrostilpnits (Feuerblende), Ag_3SbS_3. *Neues Jahrbuch für Mineralogie, Monatshefte*, **1968**, 145–160.

Laufek F., Sejkora J. and Dušek M. (2010) The role of silver in the crystal structure of pyrargyrite: single crystal X-ray diffraction study. *Journal of Geosciences*, **55**, 161–167.

Leitl M., Pfitzner A. and Bindi L. (2009) Preferred ion diffusion pathways and activation energies for Ag in the crystal structure of stephanite, Ag_5SbS_4. *Mineralogical Magazine*, **73**, 17–26.

Moëlo Y., Makovicky E., Mozgova N.N., Jambor J.L., Cook N., Pring A., Paar W., Nickel E.H., Graeser S., Karup-Møller S., Balič-Žunic T., Mumme W.G., Vurro F., Topa D., Bindi L., Bente K. and Shimizu M. (2008) Sulfosalt systematics: a review. Report of the sulfosalt sub-committee of the IMA Commission on Ore Mineralogy. *European Journal of Mineralogy*, **20**, 7–46.

Petříček V., Dušek M. and Palatinus L. (2006) *JANA2006, a crystallographic computing system*. Institute of Physics, Academy of Sciences of the Czech Republic, Prague, Czech Republic.

Rosenstingl J. and Pertlik F. (1993) Neuberechnung der kristallstruktur von natürlichem und synthetischem monoklinen Ag_3AsS_3 (= xanthokon) nebst einer discussion zur symmetrie. *Mitteilungen der Österreichischen Mineralogischen Gesellschaft*, **138**, 9–16.

Schönau K.A. and Redfern S.A.T (2002) High-temperature phase transitions, dielectric relaxation, and ionic mobility of proustite, Ag_3AsS_3, and pyrargyrite, Ag_3SbS_3. *Journal of Applied Physics*, **92**, 7415–7424.

Sheldrick G.M. (2015) Crystal structure refinement with SHELXL. *Acta Crystallographica*, **C71**, 3–8.

Voudouris P., Melfos V., Spry P.G., Bonsall T., Tarkian M. and Economou-Eliopoulos M. (2008) Mineralogical and fluid inclusion constraints on the evolution of the Plaka intrusion-related ore system, Lavrion, Greece. *Mineralogy and Petrology*, **93**, 79–110.

Wendel W. and Rieck B. (1999) Silber, Arsen und Antimon: Vererzungen im Revier Plaka (Teil 1). *Lapis*, **24**, 53–58.

Wilson A.J.C. (1992) *International Tables for Crystallography. Volume C*. Kluwer, Dordrecht, Germany.